Available online at www.sciencedirect.com

ScienceDirect

Procedia Structural Integrity 44 (2023) 1403–1410

Structural Integrity Procedia

www.elsevier.com/locate/procedia

XIX ANIDIS Conference, Seismic Engineering in Italy

Effect of ground-motion sequences on a unreinforced masonry wall restrained by an elasto-plastic tie-rod

Omar AlShawa[a,*], Fabrizio Mollaioli[a], Laura Liberatore[a], Domenico Liberatore[a], Luigi Sorrentino[a]

[a]*Sapienza Università di Roma, Dipartimento di Ingegneria Strutturale e Geotecnica, via Antonio Gramsci 53, Rome 00197, Italy.*

Abstract

This work investigates the effect of international ground-motion sequences on the out-of-plane response of an ordinary-building façade. The following assumptions are made on the wall boundary conditions: the wall is resting on a foundation, it is adjacent to transverse walls and restrained by elasto-plastic tie rods with finite elongation capacity. Four walls are considered of different aspect ratio and size; two types of masonry are assumed, and the tie is designed following a force-based procedure according to the Commentary to the Italian Building Code. The walls are modelled as rigid blocks of finite thickness and free to rotate on one side only. The rocking response of the walls, excited in the out-of-plane direction under 56 sequences of records, is evaluated. The effect of sequences is estimated by the comparison of the response experienced during the sequence and under a single record, strongest in terms of either peak ground acceleration or velocity. Finally, in order to reduce the vulnerability originated by a seismic sequence, a proposal of a reduced behaviour factor to be adopted in the design of tie rods is formulated.

Keywords: façade out of plane mechanism; force-based tie-rod design; dissipation of energy; hysteretic energy; behaviour factor

1. Introduction

Surveys after several earthquakes, e.g. the Canterbury earthquakes of 2010–2011 (Moon et al. 2014) and the Central Italy earthquakes of 2016-2017 (Mazzoni et al. 2018), show that strong ground motions often occur in sequences of main shocks of similar intensity within a very short time period. Existing masonry buildings all over the world

* Corresponding author. Tel.: +390649919189; fax: +390649919183.
E-mail address: omar.alshawa@uniroma1.it

10.1016/j.prostr.2023.01.180

exhibit significant vulnerability to earthquakes in general and may develop out-of-plane failure modes (Abrams et al. 2017; Casapulla et al. 2021; Sorrentino et al. 2014), and seismic sequences can severely affect unreinforced masonry constructions. This effect on unreinforced masonry constructions was investigated by analytical studies (AlShawa et al. 2019; Casolo 2017; Mouyiannou et al. 2014; Rinaldin and Amadio 2018). AlShawa et al. (2019) studied the effect of Italian seismic sequences by the comparison of the response experienced during the sequence and under a single record, strongest in terms of either peak ground acceleration (*PGA*) or velocity (*PGV*). Most of the sequences used to excite the model induce limited damage accumulation in the tie-rod, with exception of the 2016-2017 Central Italy earthquakes (Mollaioli et al. 2019). In order to investigate if this trend is systematic, in this paper the rocking response of the walls, excited in the out-of-plane direction by 56 international sequences of records, is evaluated. Finally, in order to reduce the vulnerability originated by a seismic sequence, a proposal of a reduced behaviour factor of tie rods is formulated for design purposes.

2. Model and ground motion features

In this work, the non-linear dynamic model of a wall excited in the out-of-plane direction and restrained by an elasto-plastic tie rods with finite elongation capacity is used (Fig. 1) (AlShawa et al. 2019). The walls are modelled as rigid blocks of finite thickness and free to rotate on one side only due to the presence of transverse structures (Fig. 1b) and are restrained by an elasto-plastic tie with limited displacement capacity. The tie can be located at any point along wall height, and it is assumed that no sliding occurs because of sufficient friction. The model accounts for a flexible base interface of given compressive strength (Fig. 1c).

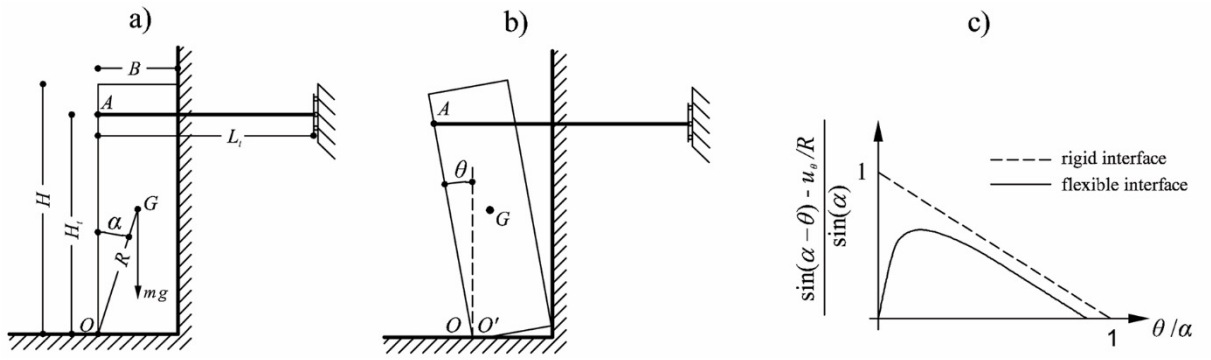

Fig. 1 Wall restrained by a tie-rod and resting on a deformable interface of finite strength. a) Geometrical parameters; b) One-sided displaced configuration on flexible interface ($\theta > 0$); c) Normalised self-weight restoring moment–rotation relationship. (AlShawa et al. 2019)

Walls characteristics

Four walls having height/thickness ratios equal to 8 or 12, and thickness equal to 0.6 or 0.9 m, and two types of masonry were considered (Table 1): a three-leaf uncut-stone masonry and a cut-stone masonry with a good bond are in accordance to the Commentary to the Italian building code (CMIT 2019). Six tie-rod normalised heights H_t/H varying from 0.5 to 1.0 are considered and, based on Podestà and Scandolo (Podestà and Scandolo 2019), three values for the steel ultimate deformation ε_u equal to 0.02, 0.06 and 0.20, are used for the numerical analyses. Tie rods were designed according to the force-based procedure established by the Italian Building Code (CMIT 2019). Earthquake return period is T_R = 500 years; *PGA* on stiff ground is a_g = 0.26 *g*; tie rod length is equal to ten times the wall thickness; prestress force is equal to ten percent of the yield one, a modern steel S235 was considered. Tie features are kept constant for all seismic sequences.

Table 1. Masonry compressive strength and bulk specific weight

Masonry type	f	w
	MPa	kN/m^3
Three-leaf uncut-stone masonry	2.5	20
Cut-stone masonry with good bond	3.2	21

Ground motion sequences

For the time history analyses 56 sequences of records, two components for 28 stations, belonging to three international seismic swarms: Mammoth Lakes (California, United States) 1980, Chi-Chi (Taiwan) 1999, and Christchurch (New Zealand) 2010-2011 have been considered. All sequences have three to six events and the selection of events defining a sequence is based on *PGV* values, because this parameter is considered to be adequately correlated with damage. All events recorded in a station and having *PGV* > 10 cm/s are included. When more than six events fulfilled the minimum *PGV* requirement the six strongest ones were retained (Table 2). The records are applied with positive and negative polarity to account for the asymmetric boundary conditions.
A plot of the sequences in terms of *PGV* is presented in Fig. 2 for both horizontal components. In all cases, a time buffer of 20 s is used between the earthquake records that are applied in sequence. The reason for using this time buffer is to ensure that the structural behaviour under the subsequent earthquake is not influenced by any remaining dynamic response to the previous earthquake.

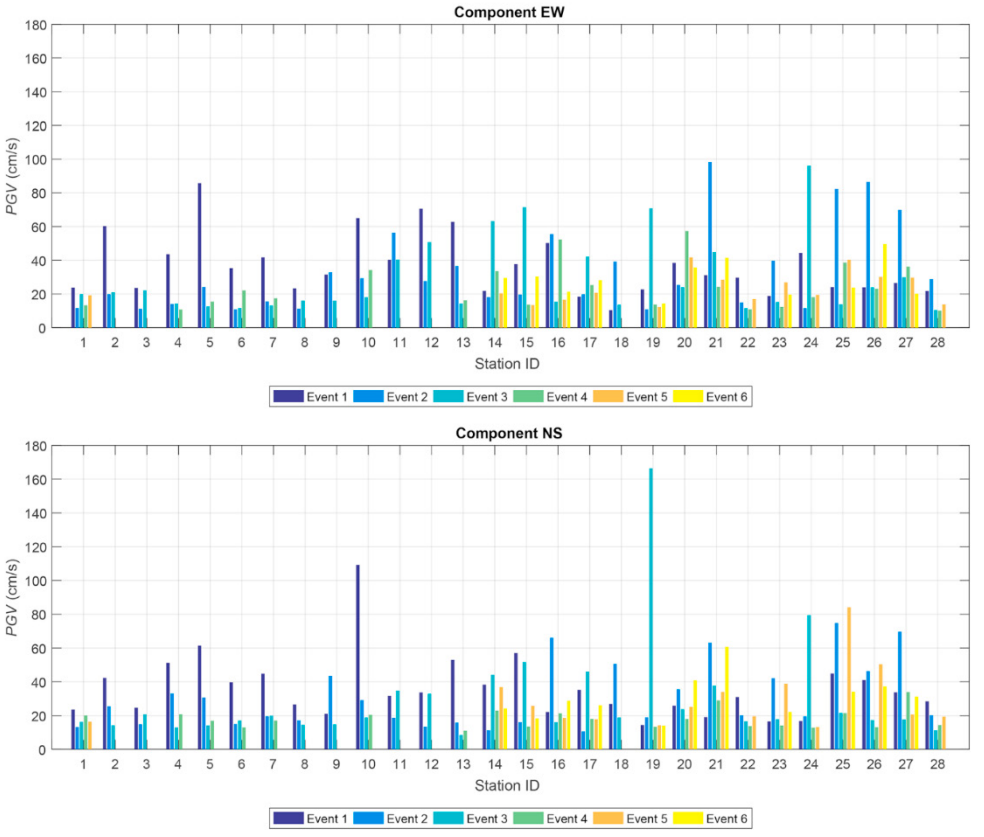

Fig. 2 Peak Ground Velocity of each event in the sequences

Table 2. List of earthquakes and selected sequences for each station

Earthquake	Event ID	Date (day-month-year)	UTC Time	M_W	ID	Station Name	Selected sequence					
							1	2	3	4	5	6
Mammoth Lakes (California, United States)	A	25/05/1980	16:34	6.06	1	Convict Creek	a	b	c	d	e	
	B	25/05/1980	16:49	5.69								
	C	25/05/1980	19:44	5.91								
	D	25/05/1980	20:35	5.70								
	E	27/05/1980	14:51	5.94								
Chi-Chi (Taiwan)	A	20/09/1999	17:47	7.62	2	CHY006	a	b	d			
	B	20/09/1999	18:03	6.20	3	CHY015	a	c	d			
	C	20/09/1999	21:46	6.20	4	CHY024	a	b	c	d		
	D	25/09/1999	23:52	6.30	5	CHY028	a	b	c	d		
					6	CHY029	a	b	c	d		
					7	CHY036	a	b	c	d		
					8	CHY047	a	c	d			
					9	CHY074	a	c	d			
					10	CHY101	a	b	c	d		
					11	TCU078	a	b	d			
					12	TCU079	a	b	d			
					13	TCU129	a	b	d			
Christchurch (New Zealand)	A	03/09/2010	16:35	7.2	14	CBGS	a	c	d	e	i	k
	B	07/09/2010	19:49	4.7	15	CCCC	a	c	d	f	k	l
	C	25/12/2010	21:30	4.7	16	CHHC	a	d	h	i	l	
	D	21/02/2011	23:51	6.2	17	CMHS	a	b	d	e	f	i
	E	22/02/2011	01:50	5.6	18	D15C	g	i	k			
	F	22/02/2011	00:04	5.5	19	GODS	g	h	i	j	k	l
	G	16/04/2011	05:49	5.0	20	HPSC	a	d	h	i	k	l
	H	13/06/2011	01:01	5.3	21	HVSC	a	d	e	f	i	
	I	13/06/2011	02:20	6.0	22	KPOC	a	d	h	i	k	
	J	15/06/2011	01:03	4.6	23	LPCC	a	d	e	f	i	k
	K	23/12/2011	00:58	5.9	24	PARS	g	i	k			
	L	23/12/2011	02:18	5.8	25	PRPC	a	d	g	i	l	
					26	REHS	a	d	e	h	i	k
					27	SHLC	a	d	h	i	k	l
					28	SMTC	a	d	e	i	k	

3. Role of the sequence

A total of 24 192 time history analyses were performed. The results are summarised in the following plots (for the sake of brevity, only the case of $\varepsilon_u = 0.20$ is shown) and tables. In order to emphasise the role (or lack thereof) of the sequence, on the vertical axis it is plotted the maximum non-dimensional rotation, θ_{max} / α, experienced during the sequence, while on the horizontal axis it is plotted the maximum non-dimensional rotation experienced under a single record, strongest in terms of either *PGA* or *PGV* (Fig. 3). If the markers are aligned along the bisector no marked sequence effect is present, although in a few instances the maximum rotation in the sequence was not recorded during the (*PGA* or *PGV*) strongest single event. If the markers depart from the bisector a sequence effect is present. Reducing the ultimate dilation, ε_u, the effect of the sequence becomes more evident. Moreover, the occurrence of overturning, marked on the boundary of the plots, increases as well, as shown in Table 3. From this table it is possible also to observe that when the tie-rod fails the wall will overturn almost systematically. Cut-stone masonry presents similar trends (Fig. 4 and Table 4).

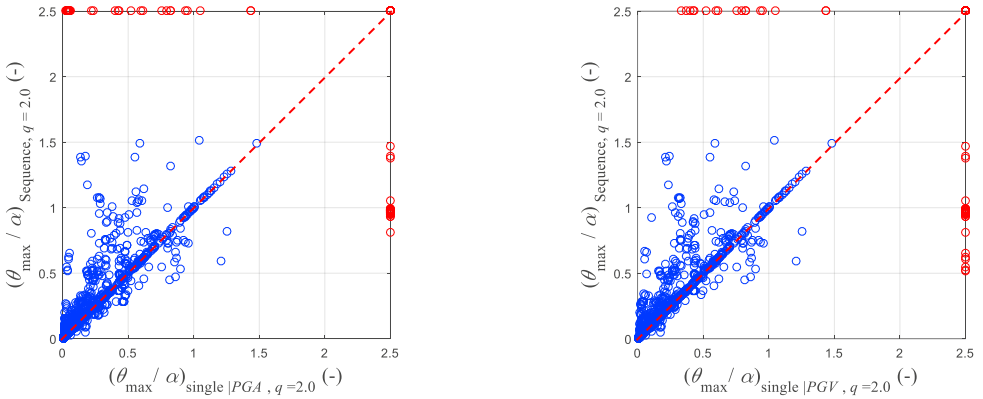

Fig. 3 Normalised maximum rotation, θ_{max} / α, of a façade with tie-rod due to the complete sequence of events or the single event having the largest: a) Peak Ground Acceleration (*PGA*); b) Peak Ground Velocity (*PGV*). Each marker is related to a wall geometry, a tie-rod height, and a sequence. Red markers lying on the boundary of the plot are related to overturned walls. Three-leaf uncut-stone masonry, $\varepsilon_u = 0.20$.

Table 3. Summary for three-leaf uncut-stone masonry (tie rod designed assuming a behaviour factor $q = 2.0$) under a complete sequence and single event having the largest Peak Ground Acceleration, *PGA* (Peak Ground Velocity, *PGV*)

ε_u	No. $\theta_{max,\ Sequence} / \theta_{max,\ Single\ \|IM}$ > 1	% ($\theta_{max,\ Sequence} / \theta_{max,\ Single\ \|IM}$)>1, excluding overturned cases	No. failed tie rods under a single event	No. failed tie rods under sequence	No. overturnings under a single event	No. overturnings under sequence
20%	777 (734)	59.2 (55.9)	33 (34)	31 (31)	33 (34)	31 (31)
6%	713 (664)	56.9 (53.0)	60 (73)	91 (91)	60 (73)	91 (91)
2%	668 (613)	67.3 (61.7)	271 (284)	362 (362)	261 (275)	351 (351)

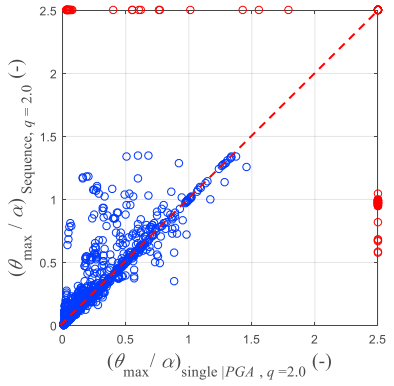

a)

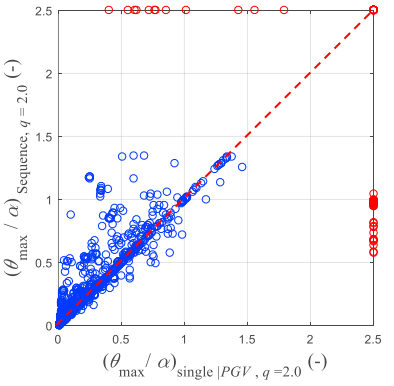

b)

Fig. 4 Normalised maximum rotation, θ_{max} / α, of a façade with tie-rod due to the complete sequence of events or the single event having the largest: a) Peak Ground Acceleration (*PGA*); b) Peak Ground Velocity (*PGV*). Each marker is related to a wall geometry, a tie-rod height, and a sequence. Red markers are lying on the boundary of the plot related to overturned walls. Cut-stone masonry with good bond, $\varepsilon_u = 0.20$.

Table 4. Summary for cut-stone masonry with good bond (tie rod designed assuming a behaviour factor q = 2.0) under a complete sequence and single event having the largest Peak Ground Acceleration, *PGA* (Peak Ground Velocity, *PGV*)

ε_u	No. $\theta_{max,\ Sequence} / \theta_{max,\ Single\|\ IM} > 1$	% ($\theta_{max,\ Sequence} / \theta_{max,\ Single\|\ IM}$)>1, excluding overturned cases	No. failed tie rods under a single event	No. failed tie rods under sequence	No. overturnings under a single event	No. overturnings under sequence
20%	828 (758)	61.6 (56.4)	7 (7)	0 (0)	7 (7)	0 (0)
6%	738 (689)	58.8 (54.9)	63 (78)	89 (89)	63 (78)	89 (89)
2%	693 (646)	69.0 (64.3)	266 (282)	351 (351)	258 (274)	340 (340)

4. Code considerations

In order to reduce the vulnerability originated by a seismic sequence, the tie rod was designed also with a reduced behaviour factor, q = 1.5.

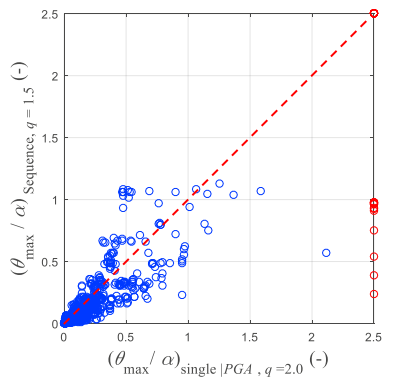

a)

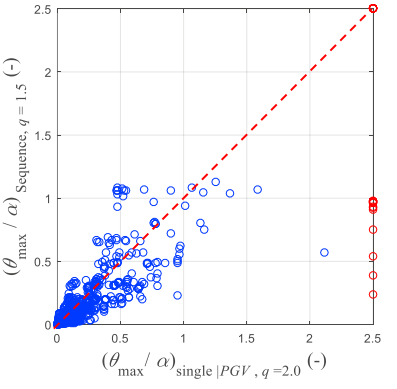

b)

Fig. 5 Normalised maximum rotation, θ_{max} / α, of a façade with tie-rod designed according to a behaviour factor $\boldsymbol{q = 1.5}$ under a complete sequence of events and tie-rod designed according to a behaviour factor q = 2.0 under a single event having the largest: a) Peak Ground Acceleration (*PGA*); b) Peak Ground Velocity (*PGV*). Each marker is related to a wall geometry, a tie-rod height, and a sequence. Red markers are lying on the boundary of the plot related to overturned walls. **Three-leaf uncut-stone masonry**, $\varepsilon_u = 0.20$.

Table 5. Summary for three-leaf uncut-stone masonry (tie rod designed according to a behaviour factor $\boldsymbol{q}$ **= 1.5**) under a complete sequence and single event having the largest Peak Ground Acceleration, *PGA* (Peak Ground Velocity, *PGV*)

$\boldsymbol{\varepsilon_u}$	No. $\theta_{max,\ Sequence}$ / $\theta_{max,\ Single\mid IM} > 1$	% ($\theta_{max,\ Sequence}$ / $\theta_{max,\ Single\mid IM}$)>1, excluding overturned cases	No. failed tie rods under a single event	No. failed tie rods under sequence	No. overturnings under a single event	No. overturnings under sequence
20%	145 (165)	11.0 (12.5)	38 (38)	24 (24)	38 (38)	24 (24)
6%	256 (254)	19.9 (19.7)	60 (73)	55 (55)	60 (73)	55 (55)
2%	250 (242)	22.5 (21.7)	271 (284)	237 (237)	261 (275)	231 (231)

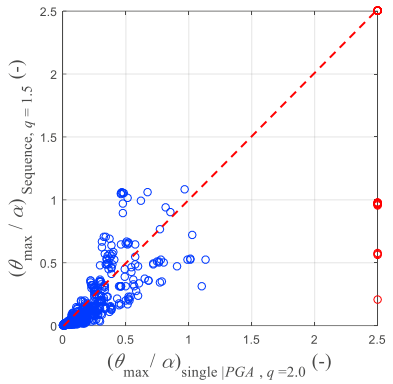

a)

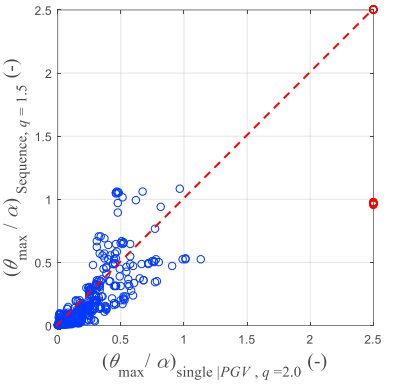

b)

Fig. 6 Normalised maximum rotation, θ_{max} / α, of a façade with tie-rod designed according to a behaviour factor $\boldsymbol{q}$ **= 1.5** under a complete sequence of events and tie-rod designed according to a behaviour factor q = 2.0 under a single event having the largest: a) Peak Ground Acceleration (*PGA*); b) Peak Ground Velocity (*PGV*). Each marker is related to a wall geometry, a tie-rod height, and a sequence. Red markers are lying on the boundary of the plot related to overturned walls. **Cut-stone masonry with good bond**, $\varepsilon_u = 0.20$.

Table 6. Summary for cut-stone masonry with good bond (tie rod designed according to a behaviour factor $\boldsymbol{q}$ **= 1.5**) under a complete sequence and single event having the largest Peak Ground Acceleration, *PGA* (Peak Ground Velocity, *PGV*)

$\boldsymbol{\varepsilon_u}$	No. $\theta_{max,\ Sequence}$ / $\theta_{max,\ Single\mid IM} >$ 1	% ($\theta_{max,\ Sequence}$ / $\theta_{max,\ Single\mid IM}$)>1, excluding overturned cases	No. failed tie rods under a single event	No. failed tie rods under sequence	No. overturnings under a single event	No. overturnings under sequence
20%	246 (260)	18.6 (19.7)	31 (31)	24 (24)	31 (31)	24 (24)
6%	267 (258)	20.7 (20.0)	63 (78)	57 (57)	63 (78)	57 (57)
2%	259 (255)	23.0 (22.6)	266 (282)	223 (223)	258 (274)	216 (216)

Then, the wall performance under the sequence in terms of normalised maximum rotation was compared with that of the same wall with a tie rod designed for q = 2.0 under the single largest record of the sequence, selected according to *PGA* or *PGV*. In Fig. 5 (for the sake of brevity, only the case of $\varepsilon_u = 0.20$ is included) it is possible to observe an enhanced symmetry about the bisector and a reduced number of overturnings (Table 5). Similar trends are again observed for a cut-stone masonry with good bond (Fig. 6 and Table 6). This approach could be pursued whenever there is a substantial probability of a sequence of earthquakes, the probability to be defined in specific hazard studies.

5. CONCLUSIONS

This paper investigates the effect of ground-motion sequences on the out-of-plane response of an ordinary-building façade. To this aim, numerical analyses are performed considering four walls of different aspect ratio and size. Two masonry compressive strengths, related to two different masonry types, namely a three-leaf uncut-stone masonry and a cut-stone masonry with good bond, are assumed. The walls are resting on a foundation, are adjacent to transverse walls, and restrained by an elasto-plastic tie rod with finite elongation capacity. The tie is designed following a force-based procedure according to the Commentary to the Italian Building Code. Three values for the steel ultimate deformation ε_u are considered for the numerical analyses. The walls are modelled as rigid blocks of

finite thickness and are free to rotate on one side only. The rocking response of the walls, in terms of maximum normalised rotations and number of overturnings, excited in the out-of-plane direction under 56 international sequences of records, is evaluated. The effect of sequences is estimated by the comparison of the response experienced during the sequence and under a single record, strongest in terms of either peak ground acceleration or velocity. As expected, the effect of the sequence is marked, especially for low values of the ultimate dilation, ε_u, in which case the effect of the sequence becomes more evident.
Finally, the effect of reducing the behaviour factor used for the tie-rod design is investigated. It is found that the reduction of such factor improves the response of the walls under earthquake sequences with a substantial decrease of the normalised rotations and of the number of overturnings. Therefore, the use of a reduced behaviour factor is suggested in the tie-rod design, so as to spare expensive non-linear time history analyses, provided that hazard studies account for sequences of multiple earthquakes and not just maximum events. Future research should involve extensions of the presented model, accounting for degradation of masonry at wall anchor, in order to capture damage accumulation in the masonry and not only in the steel.

Acknowledgements

This work was partially carried out within the research project SISTINA (SIStemi Tradizionali e INnovativi di tirantatura delle Architetture storiche) funded by Sapienza University of Rome, and partially funded by the 'Dipartimento di Protezione Civile – Consorzio RELUIS' program. The opinions expressed in this publication are those of the authors and are not necessarily endorsed by the funding bodies.

References

Abrams, D. P., AlShawa, O., Lourenço, P. B., Sorrentino, L., 2017. Out-of-Plane Seismic Response of Unreinforced Masonry Walls: Conceptual Discussion, Research Needs, and Modeling Issues. International Journal of Architectural Heritage. 11, 22–30. doi: 10.1080/15583058.2016.1238977

AlShawa, O., Liberatore, D., Sorrentino, L., 2019. Dynamic One-Sided Out-Of-Plane Behavior of Unreinforced-Masonry Wall Restrained by Elasto-Plastic Tie-Rods. International Journal of Architectural Heritage. 13, 340–357. doi: 10.1080/15583058.2018.1563226

AlShawa, O., Liberatore, L., Liberatore, D., Mollaioli, F., Sorrentino, L., 2019. Seismic Demand on a Unreinforced Masonry Wall Restrained by Elasto-Plastic Tie-Rods Under Earthquake Sequences. International Journal of Architectural Heritage. 13, 1124–1141. doi: 10.1080/15583058.2019.1645239

Casapulla, C., Argiento, L. U., Maione, A., Speranza, E., 2021. Upgraded formulations for the onset of local mechanisms in multi-storey masonry buildings using limit analysis. Structures. 31, 380–394. doi: 10.1016/j.istruc.2020.11.083

Casolo, S., 2017. A numerical study on the cumulative out-of-plane damage to church masonry façades due to a sequence of strong ground motions. 46, 2717–2737. doi: 10.1002/eqe.2927

CMIT., 2019. Instruction for the application of the Building Standard for Constructions. G.U. n. 35 del 11-2-2019. Suppl. Ordinario n.5 – Circolare 21 gennaio 2019, n. 7 C.S.LL.PP.; 2019 [in Italian]

Mazzoni, S., Castori, G., Galasso, C., Calvi, P., Dreyer, R., Fischer, E., Fulco, A., Sorrentino, L., Wilson, J., Penna, A., Penna, A., Magenes, G., 2018. 2016-2017 central Italy earthquake sequence: Seismic retrofit policy and effectiveness. Earthquake Spectra. 34, 1671–1691. doi: 10.1193/100717EQS197M

Mollaioli, F., AlShawa, O., Liberatore, L., Liberatore, D., Sorrentino, L., 2019. Seismic demand of the 2016–2017 Central Italy earthquakes. Bulletin of Earthquake Engineering. 17, 5399–5427. doi: 10.1007/s10518-018-0449-y

Moon, L., Dizhur, D., Senaldi, I., Derakhshan, H., Griffith, M., Magenes, G., Ingham, J., 2014. The demise of the URM building stock in Christchurch during the 2010-2011 Canterbury earthquake sequence. Earthquake Spectra. 30, 253–276. doi: 10.1193/022113EQS044M

Mouyiannou, A., Penna, A., Rota, M., Graziotti, F., Magenes, G., 2014. Implications of cumulated seismic damage on the seismic performance of unreinforced masonry buildings. Bulletin of the New Zealand Society for Earthquake Engineering. 47, 157–170. doi: 10.5459/bnzsee.47.2.157-170

Podestà, S., Scandolo, L., 2019. Earthquakes and Tie-Rods: Assessment, Design, and Ductility Issues. International Journal of Architectural Heritage. 13, 329–339. doi: 10.1080/15583058.2018.1563239

Rinaldin, G., Amadio, C., 2018. Effects of seismic sequences on masonry structures. Engineering Structures. 166, 227–239.

Sorrentino, L., Alshawa, O., Liberatore, D., 2014. Observations of Out-of-Plane Rocking in the Oratory of San Giuseppe Dei Minimi during the 2009 L'Aquila Earthquake. Applied Mechanics and Materials. 621, 101–106. doi: 10.4028/www.scientific.net/AMM.621.101